Theor Chem Acc (2009) 123:443–453
DOI 10.1007/s00214-009-0555-7

REGULAR ARTICLE

Density functional study on rare gas-noble metal closed-shell interaction in XeMX (M = Au, Ag, Cu; X = F, Cl, Br) systems

Hua Fang · Xiao-Gang Zhang

Received: 12 November 2008 / Accepted: 26 February 2009 / Published online: 17 March 2009

Abstract The rare gas-noble metal systems XeMX (M = Au, Ag, Cu; X = F, Cl, Br) were investigated at the CCSD(T) and DFT levels. Geometric structures, natural bond orbital population, HOMO-LUMO gap, the rare gas-noble metal interaction and the chemical deformation density were analyzed. Experimental structure parameters of the XeAuF and XeMX (M = Ag, Cu; X = F, Cl) were reproduced at Xα level. At the same time, the XeAuCl and XeMBr (M = Au, Ag, Cu) compounds were predicted. The electronegativity of halogen atom X correlates with the M–X bond length, HOMO-LUMO gap, electronic structures and Xe–M bond energy.

Keywords Density functional · Rare gas-noble metal bonding · NBO population · Chemical deformation density

1 Introduction

In 1933, Pauling [1] anticipated the possibility of formation of stable molecules involving rare gas atoms. Four decades later, his prediction became a reality through the preparation [2] of xenon hexafluoroplatinate [$Xe^{+}(PtF_6)^{-}$], the first compound containing a rare gas atom. In the recent years, chemical compounds involving rare gas elements have attracted considerable attention [3–5] from experimentalists as well as theoreticians. They are gradually discovered and well investigated in experiment with a high-resolution Fourier transform microwave spectrometer [6–18]. This kind of novel compound with rare gas elements exists and is of considerable significance to open up the new fascinating field in the physics and chemistry. Recently, Seidel and Seppelt [19] demonstrated the existence of the $[AuXe_4]^{2+}$ cation in crystal structure of the $AuXe_4{}^{2+}[Sb_2F_{11}{}^{-}]_2$ compound. The work is very important because it supports the concept that the rare gas atoms can be directly bonded to the gold atom. In these species, the presence of chemical bonds between gold and xenon is in sharp contrast to the conventional behavior of rare gas and noble metal atoms, which are considered to be inert from the existing chemical intuitions. Between rare gas atom and noble-metal halides, the interaction also can be thought as two closed-shell (for example: in XeAuF system, Xe: $5p^6$, Au(I): $5d^{10}$) fragments interaction.

For the closed-shell interaction, where dispersion interaction plays an important role, it was thought that DF methods are not applicable. However, there is now much evidence that a careful choice of the DF gives reasonable bond lengths and bond energies of Au(I) cluster systems [20–24]. Whether DF methods can be fit for such special interaction between rare gas and noble metal? Otherwise, Pyykkö [25, 26] suggested that most of the bonding interaction in NgMX is covalent in character; the interpretation was questioned by saying that "covalency within the $NgAu^{+}$ species appears to be unproven" [27]. The second goal for us is to know which kind of the rare gas-noble metal interaction is.

Here, we reported the elementary results on closed-shell interaction system XeMX. The theoretical investigations by using DF methods including geometrical structures, electronic structures in such special closed-shell interaction system are less reported. In the present research, the investigations of the XeMX (M = Au, Ag, Cu; X = F, Cl, Br) series are not only to understand the behavior of the systems

H. Fang (✉) · X.-G. Zhang
College of Material Science and Technology,
Nanjing University of Aeronautics and Astronautics,
210016 Nanjing, People's Republic of China
e-mail: susanfang@nuaa.edu.cn

Table 1 Calculated structural parameters of XeMX (distances in pm)

Method	XeAuF		XeAuCl		XeAuBr	
	R_{Xe-Au}	R_{Au-F}	R_{Xe-Au}	R_{Au-Cl}	R_{Xe-Au}	R_{Au-Br}
MP2[a]	254.5	192.2	259.8	221.3		
MP2[b]	254.2					
MP2[c]	255.0					
MP2[d]	251.2	190.1				
CCSD(T)[d]	257.3	192.1				
CCSD(T)	256.3	192.9	261.8	223.1	263.6	234.4
Xα	254.0	191.6	260.0	220.9	261.1	234.7
VWN	254.0	191.4	258.6	220.3	259.6	234.1
VBP	261.7	195.7	267.7	224.8	270.0	239.1
VPW91	261.3	195.6	267.1	224.8	269.5	238.9
Exp.[e]	254.3	191.8				
R^f_{cov}	257.0		257.0		257.0	
R^f_{vdW}	295.0		295.0		295.0	
Method	XeAgF		XeAgCl		XeAgBr	
	R_{Xe-Ag}	R_{Ag-F}	R_{Xe-Ag}	R_{Ag-Cl}	R_{Xe-Ag}	R_{Ag-Br}
MP2[a]	268.4	196.9	272.8	227.4		
MP2[b]	266.5					
MP2[c]	268.0		273.0			
CCSD(T)	265.7	196.4	270.1	227.7	271.8	238.9
Xα	266.0	195.9	267.0	226.4	266.2	239.1
VWN	265.8	194.9	266.8	225.4	266.1	238.1
VBP	275.1	200.0	282.0	231.2	285.0	245.1
VPW91	274.9	199.9	281.4	231.2	284.3	244.6
Exp.[e]	266.2	197.1	270.0			
R^f_{cov}	258.0		258.0		258.0	
R^f_{vdW}	299.0		299.0		299.0	
Method	XeCuF		XeCuCl		XeCuBr	
	R_{Xe-Cu}	R_{Cu-F}	R_{Xe-Cu}	R_{Cu-Cl}	R_{Xe-Cu}	R_{Cu-Br}
MP2[a]	245.9	173.7	249.7	206.6		
MP2[b]	243.9					
MP2[c]	246.0		250.0			
CCSD(T)	242.9	174.3	246.9	206.0	248.5	218.2
Xα	243.0	173.6	249.0	204.8	249.9	218.5
VWN	243.0	173.4	243.4	204.3	247.1	218.2
VBP	253.3	177.0	258.8	208.4	260.8	222.7
VPW91	253.4	177.2	258.6	208.5	259.8	222.6
Exp.[e]	243.0	175.0	247.0			
R^f_{cov}	237.0		237.0		237.0	
R^f_{vdW}	278.0		278.0		278.0	

[a] The results from Ref. [52]

[b] The results from Ref. [53]

[c] The results from Ref. [12] for XeAuF; Ref. [13] for XeAgF and XeAgCl; Ref. [16] for XeCuF and XeCuCl

[d] The results from Ref. [54] for XeAuF

[e] The experimental values for XeAuF in Ref. [12]; for XeAgF and XeAgCl in Ref. [13]; for XeCuF and XeCuCl in Ref. [16]

[f] The terms R_{cov} and R_{vdW} indicate the covalent and van der Waals limits, respectively, of the Xe–M bond (see text for more details), in Refs. [16] and [18]

under consideration, but also to give an insight into the nature of the bond between rare gas and noble metal atoms. It would be meaningful and interesting to give a description of structures and properties of this new class of compounds.

2 Computational details

The geometries were optimized by the CCSD(T) and DFT methods. The CCSD(T) calculations were carried out with the program packages GAUSSIAN 03 [28] and DFT calculations were performed with ADF 2008 package initially developed by Baerends et al. [29]. Several different DFT potentials of exchange-correlation were carried out to the systems. We used: (1) the simple local Xα exchange potential by Slater [30–33], with parameter $\alpha = 0.7$; (2) the local correlation-corrected version developed by Vosko, Wilk and Nusair (VWN) in 1980 [34]; (3) the nonlocal gradient exchange potential of Becke (B) of 1988 [35] and the nonlocal gradient correlation potential of Perdew (P) of

1986 [36]; (4) the generalized gradient approach of Perdew and Wang (PW91)[37] and their combinations.

Because the dominating interactions in chemical process mainly come from the valence electrons, and in order to reduce the calculation costs the inner core shells were frozen via a frozen approximation [38], namely [$1s^2$] for F, [$1s^2$–$2p^6$] for Cl, [$1s^2$–$3d^{10}$] for Br, [$1s^2$–$4f^{14}$] for Au, [$1s^2$–$4p^6$] for Ag, [$1s^2$–$3p^6$] for Cu and [$1s^2$–$4d^{10}$] for Xe. All of the core electrons were calculated by Dirac method [39] and unchanged transferred into molecules. Relativistic effects were particularly important. The zeroth order regular approximation scalar Hamiltonian [40–44] was adopted.

The higher level TZ2P-STO basis sets for all atoms were used in DFT calculations. In ab initio CCSD(T) calculations, the aug-cc-PVTZ basis sets [45–51] for F, Cl, Br, Au, Ag, Cu and Xe atoms. For Au, Ag, Cu and Xe atoms, the corresponding atom-centered effective core potentials were used [48, 49]. All structures were fixed to a linear configuration.

3 Results and discussions

3.1 Structures of the molecules

The important property of the rare gas-noble metal halides is perhaps the short rare gas-to-metal bond length. This property was first noticed with ArAgCl [6] and continues to be observed in all other NgMX molecules. Table 1 shows the experimental, ab initio and DFT structural parameters for XeMX (M = Au, Ag, Cu; X = F, Cl, Br) molecules. It is interesting to compare the rare gas-noble metal bond lengths as obtained in the present work with that of earlier reports for different classes of rare gas compounds [12, 13, 16, 52–54] containing noble metal-rare gas bonding.

For XeAuF, high level CCSD(T) with high-quality basis sets overestimated the Xe–Au distance by 2 pm compared to the experimental values. Local density functional (VWN, Xα) reproduce the Xe–Au distance. While the nonlocal exchange correlation corrections (VBP, VPW91)were added, the Xe–Au distance were overestimated 7 pm. Recently, Belpassi et al. [54] have studied NgAuF and $NgAu^+$ systems (Ng = Ar, Kr, Xe) by using all-electron fully relativistic DC-CCSD(T) method with high-quality extended basis sets, which has 1 g function. For XeAuF system, the obtained Xe–Au bond length is 3 pm above experiment. Our Xα method gave the even better results. For XeMX (M = Ag, Cu; X = F, Cl) systems, the Xe–M distances obtained by CCSD(T) are consistent with the experimental values within 1 pm. Local density functional (VWN, Xα) reproduce the Xe–M distance. The Xα gave the same good results with the CCSD(T). While the nonlocal exchange correlation corrections (VBP, VPW91) were added, the Xe–M distance was overestimated by about 10 pm. For XeMX (M = Au, Ag, Cu; X = F, Cl, Br) molecules, the bond lengths are quite short in comparison to those of the van der Waals complexes Ar–NaCl [55], ArHg [56], Kr–HF [57], and Xe–HF [58]. The short bond lengths are reproduced by both ab initio CCSD(T) and LDF–Xα calculations.

In view of the interesting reports [6–8, 12, 14, 15] on comparison of the Xe–M bond length with respect to a covalent limit R_{cov} [r_{cov}(M(*I*)) + r_{cov}(Ng)] and a van der Waals limit R_{vdW}[$r_{ion}(M^+)$+r_{vdW}(Ng)]. Both of these limits are simply benchmark values and should not be considered as hard and fast rules. We have tabulated the corresponding limiting values of the bond lengths in Table 1. From this table, it is quite evident that the calculated Xe–Ag and Xe–Cu bond lengths are less than the van der Waals limits and greater than the covalent limits. However, Xe–Au distance is less than the covalent limit.

The values for the stretching frequencies for several XeMX molecules are given in Table 2.

The low values in all cases indicate that the complexes are rigid. They are much more rigid than the reference van der Waals complex Ar–NaCl [55]. From the comparison in Table 2, it is clear that the ω(XeM) frequencies in XeMX complexes decreased when the halogen atom changes from F to Br. In all cases, these frequencies are much greater than the ω(ArNa) value for the Ar–NaCl van der Waals bond, and much nearer to low-end values for chemical bonds.

3.2 NBO population of XeMX (M = Au, Ag, Cu; X = F, Cl, Br)

Second, we discuss the charge distributions in XeMX systems by means of natural bond orbital (NBO)

Table 2 Harmonic Frequencies ω_e (cm^{-1}) of the Xe–M Bond in XeMX

Complex	ω(NgM) (cm^{-1})			ω(MX) (cm^{-1})
	Cal.[a]	Cal.[b]	Exp.[c]	Cal.[a]
XeAuF	177.72	165.00	169.00	599.00
XeAuCl	154.00			390.76
XeAuBr	142.74			270.86
XeAgF	135.08	108.00	130.00	530.50
XeAgCl	132.59	99.00	120.00	353.83
XeAgBr	123.87			266.10
XeCuF	184.23	169.00	178.00	652.03
XeCuCl	153.46	146.00	155.00	427.27
XeCuBr	131.43			330.62
Ar–NaCl	21.00[d]			

[a] This work

[b] The results from Ref. [12] for XeAuF, Ref. [13] for XeAgF and XeAgCl; Ref. [16] for XeCuF and XeCuCl

[c] Experimental values from Table 5 in Ref. [12]

[d] Ref. [55]

Table 3 NBO populations and charges of XeMX at Xα level

System	Xe5s	Xe5p	Mns[a]	Mnp[a]	M($n-1$)d[a]	Q_{Xe}	Q_M	Q_X
XeAuF	1.97	5.76	0.84	0.03	9.69	0.24	0.42	−0.66
XeAuCl	1.97	5.79	0.86	0.03	9.78	0.21	0.30	−0.51
XeAuBr	1.97	5.79	0.89	0.04	9.82	0.22	0.23	−0.45
XeAgF	1.98	5.86	0.46	0.02	9.86	0.14	0.64	−0.78
XeAgCl	1.98	5.87	0.54	0.02	9.90	0.14	0.52	−0.66
XeAgBr	1.98	5.86	0.57	0.03	9.91	0.14	0.46	−0.60
XeCuF	1.98	5.85	0.52	0.05	9.79	0.15	0.62	−0.77
XeCuCl	1.98	5.86	0.56	0.05	9.86	0.15	0.52	−0.67
XeCuBr	1.98	5.86	0.59	0.05	9.89	0.15	0.46	−0.61

[a] For Au $n = 6$, for Ag $n = 5$, for Cu $n = 4$

population analysis. Corresponding results are shown in Table 3. The atomic charges vary systematically, in the case of Au by about 0.2 from +0.42 for strongly electronegative F to +0.23 for least electronegative Br. So do the atomic charges of Ag and Cu atom. At the same time, there are about 0.1–0.2 electron holes in the M($n-1$)d and Xe5p semi-core shell, while the outer valence shell is still populated by 0.5–0.8e in the Mns and approximately 2.0e in Xe5s shell. Ag4d shell transfers a few electrons to Ag5sp shell. Since Xe5p and M($n-1$)d shell is not completely closed shell, the weak rare gas-noble metal interaction occurs. The quantum calculation indicated a net charge transfer of ~0.15 electron from Xe to MX, as well as valence molecular orbital with fully shared electron density between Xe and M. There is thus strong evidence of rare gas-noble metal chemical bonding in these complexes.

3.3 Xe–M bond energy decomposition

Thirdly, the Xe–M bond energy has been analyzed and decomposed. According the theory of Ziegler [59], the bond energy can be split up into two parts [60, 61]. One is the "steric interaction energy" ($E_{ster.}$) that comes from the electrostatic interaction ($E_{ele.}$) between the fragments (with unchanged electron densities) and the Pauli exchange repulsion (E_{pauli}) due to the antisymmetry requirement raising the energy when occupied fragment orbitals overlap. The other is the "orbital interaction energy" ($E_{orb.}$) due to quantum mechanical interference and orbital relaxation from the initial fragment states to the final molecular states. The orbital interaction contains charge transfer contributions (mixing of occupied orbitals on one fragment and virtual orbitals on the other fragment) and polarization contributions (mixing of occupied and virtual orbitals on the fragment itself). The bond energies are analyzed and presented in Table 4.

$$E_{tot.} = E_{ster.} + E_{orb.} = E_{Pauli} + E_{ele.} + E_{orb.} \quad (1)$$

The Xe–M bonding energy for the XeMX at the Xα level are broken down following the Eq. 1 and given in Table 4. For XeMX systems, when the Xe and MX approach each other, the Pauli overlap repulsion increases comparatively slowly, whereas the electrostatic overlap attraction increases significantly enough so that the combined effect of orbital mixing and electron correlation adds up to a weak interaction.

Interesting trends so far observed include the increasing strength of the Xe–M interaction in XeMX as X is altered from Br to F. A traditional viewpoint recognizes these trends as being consistent with the greater electron withdrawing properties of F over Cl. The relationship between the Xe–M interaction energy and the electronegativity of X is linear (Table 5; Fig. 1). At the same time, we observed the increasing strength of the Xe–M interaction in XeMX is along with the order: $E_{Xe-Au} > E_{Xe-Cu} > E_{Xe-Ag}$. Our calculated results are consistent with the results in [6–8, 12, 14, 15, 52].

Table 4 Xe–M interaction energy $\Delta E_{tot.}$ (in kJ/mol) decomposition of XeMX at Xα level

System	E_{pauli}	$E_{ele.}$	$E_{pauli} + E_{ele.}$	$E_{orb.}$	$\Delta E^a_{tot.}$
XeAuF	+244.69	−206.08	+38.61	−168.08	−129.47
XeAuCl	+223.76	−185.11	+38.65	−143.39	−104.74
XeAuBr	+226.58	−185.75	+40.83	−139.03	−98.20
XeAgF	+124.10	−116.75	+7.35	−78.73	−71.38
XeAgCl	+132.68	−117.96	+14.72	−74.64	−59.92
XeAgBr	+144.92	−125.35	+19.57	−75.73	−56.16
XeCuF	+137.25	−122.08	+15.17	−105.14	−89.97
XeCuCl	+126.28	−112.49	+13.79	−90.82	−77.03
XeCuBr	+133.12	−117.37	+15.75	−89.75	−74.00

[a] $\Delta E_{tot.}$ represents the Xe–M bong energy

Table 5 The Pauling electronegativity (EN_χ), M–X bond length R_{M-X} (in pm), the HOMO-LUMO gap $\Delta\varepsilon_i$ (in eV) and the Xe–M bond energy of $\Delta E_{tot.}$ (in kJ/mol) in the XeMX system

System	EN_χ	R_{M-X}	$\Delta\varepsilon_i$	$\Delta E^a_{tot.}$
XeAuF	3.90	191.6	3.93	−129.47
XeAuCl	3.16	220.9	3.56	−104.74
XeAuBr	2.96	234.7	3.26	−98.20
XeAgF	3.90	195.9	3.74	−71.38
XeAgCl	3.16	226.4	3.50	−59.92
XeAgBr	2.96	239.1	3.28	−56.16
XeCuF	3.90	173.6	3.74	−89.97
XeCuCl	3.16	204.8	3.65	−77.03
XeCuBr	2.96	218.5	3.47	−74.00

[a] $\Delta E_{tot.}$ represents the Xe–M bong energy

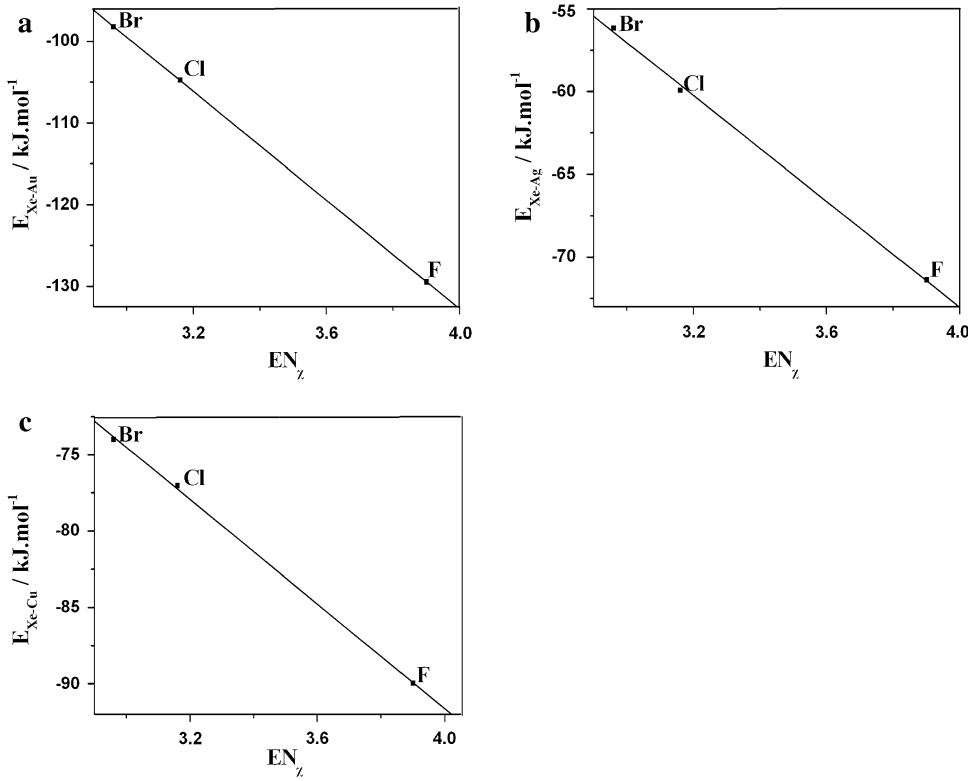

Fig. 1 Electronegativity EN_χ of atom X plotted against Xe–M bond energy ($E_{Xe–M}$) in **a** XeAuX; **b** XeAgX; **c** XeCuX

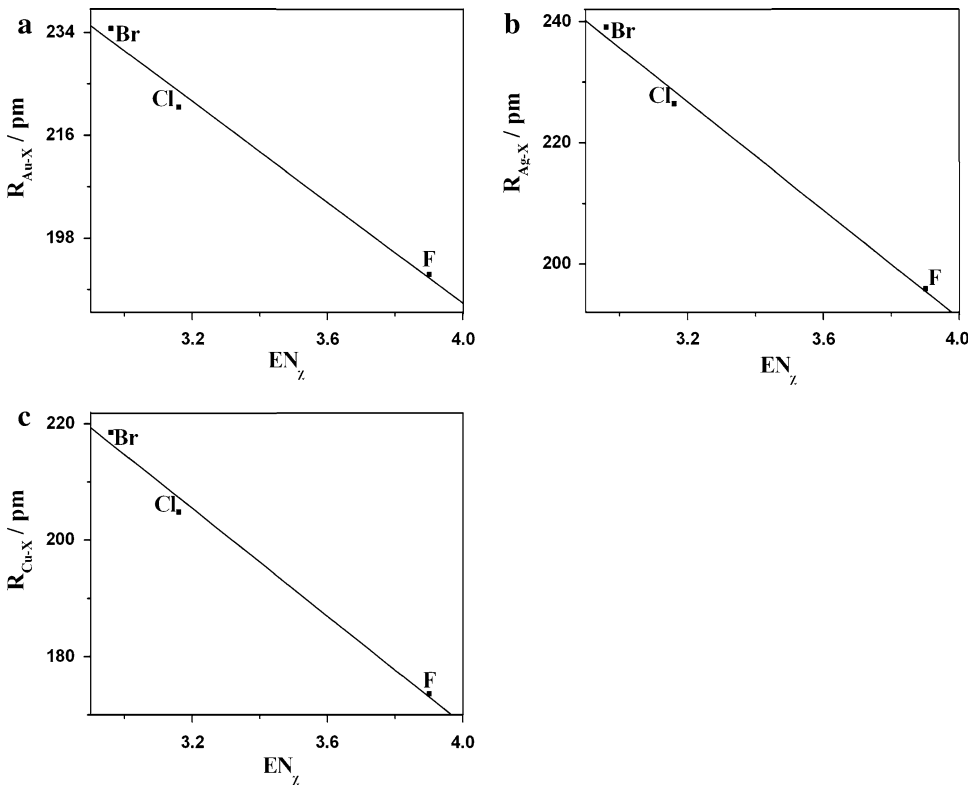

Fig. 2 Electronegativity EN_χ of halide atom X plotted against M–X bond length ($R_{M–X}$) in **a** XeAuX; **b** XeAgX; **c** XeCuX

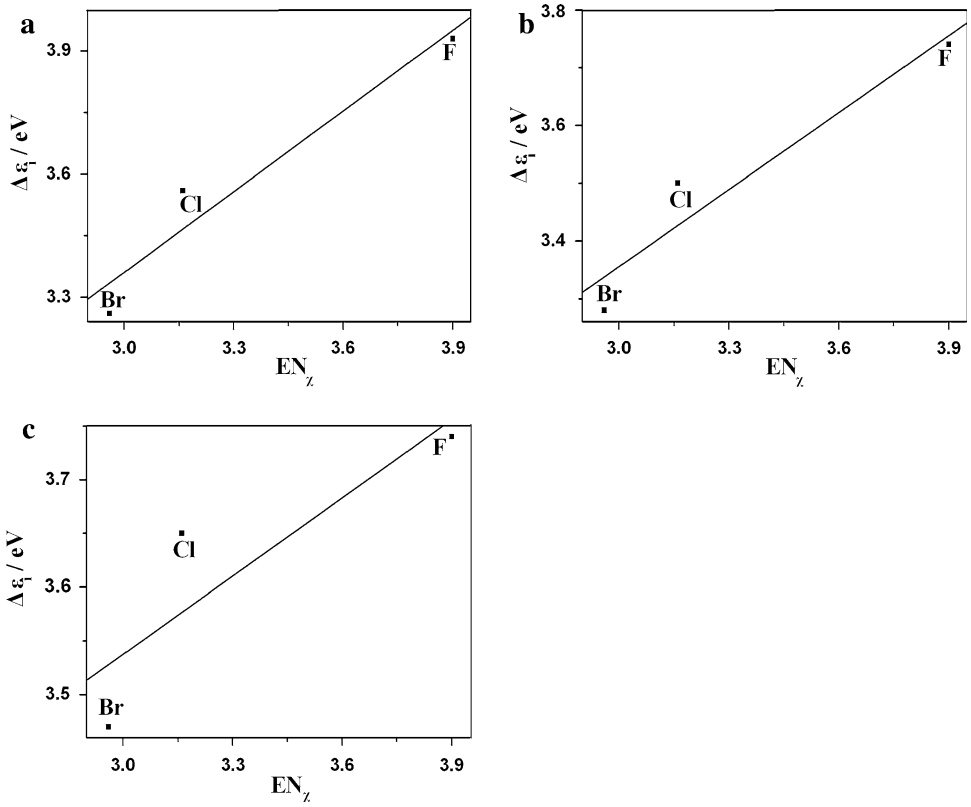

Fig. 3 Electronegativity (EN_χ) of atom X plotted against HOMO-LUMO gap ($\Delta\varepsilon_i$) in **a** XeAuX; **b** XeAgX; **c** XeCuX

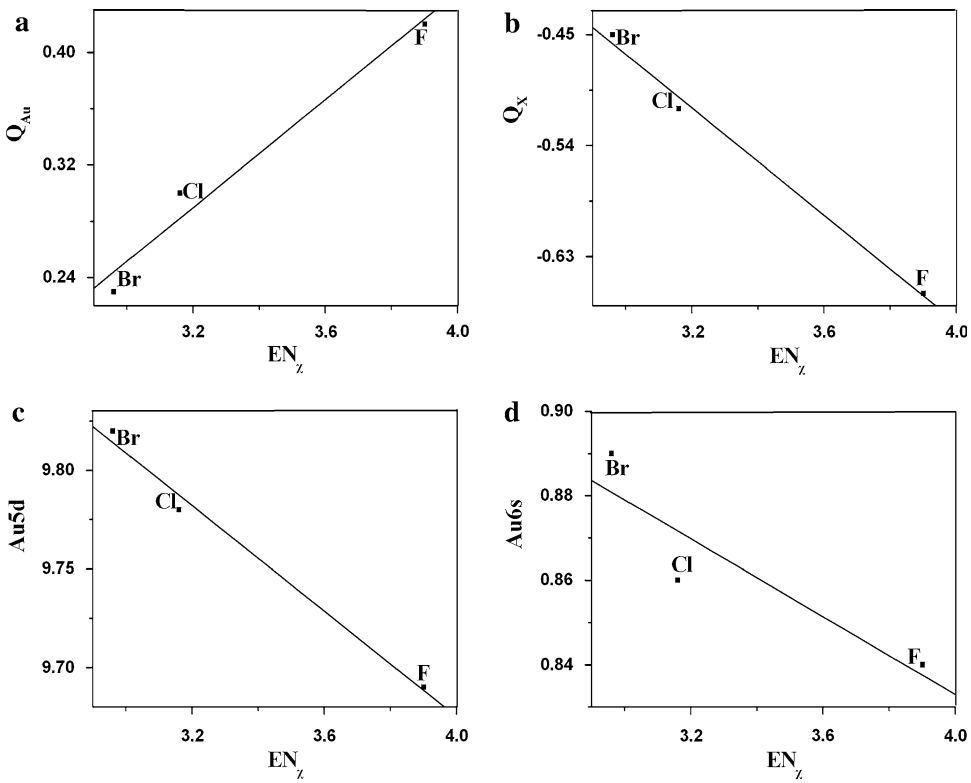

Fig. 4 Correlation of electronegativity EN_χ of atom and, **a** effective charge of Au, Q_{Au}; **b** effective charge of X, Q_X; **c** population of Au5d; **d** population of Au6s in XeAuX

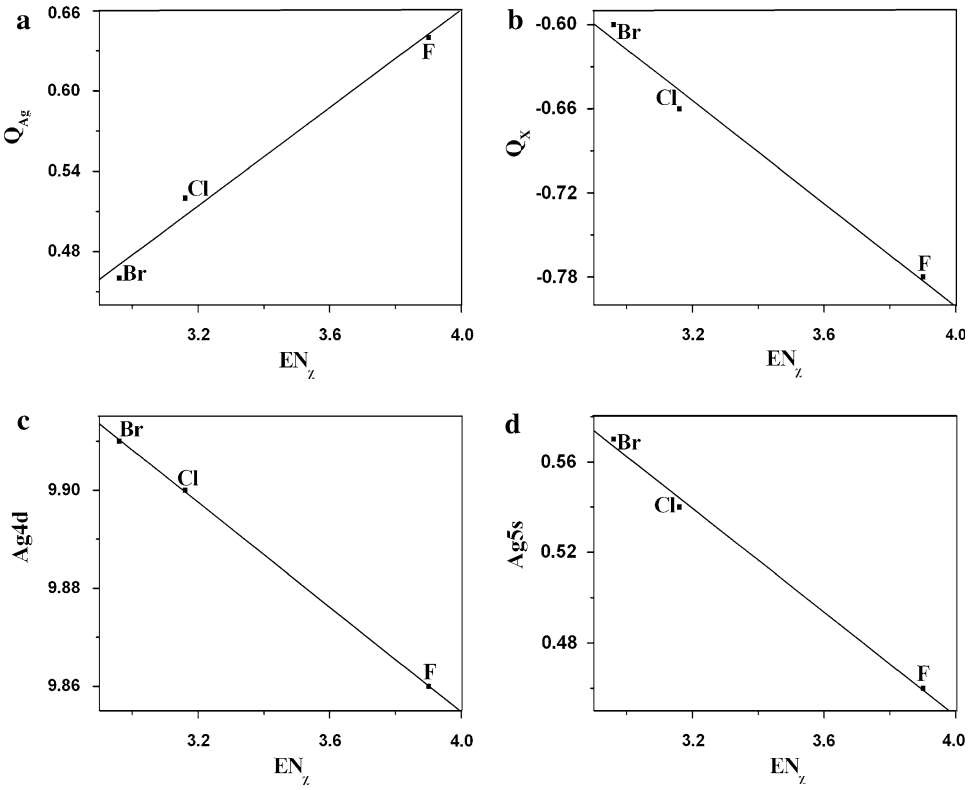

Fig. 5 Correlation of electronegativity EN_χ of atom and, **a** effective charge of Ag, Q_{Ag}; **b** effective charge of X, Q_X; **c** population of Ag4d; **d** population of Ag5s in XeAgX

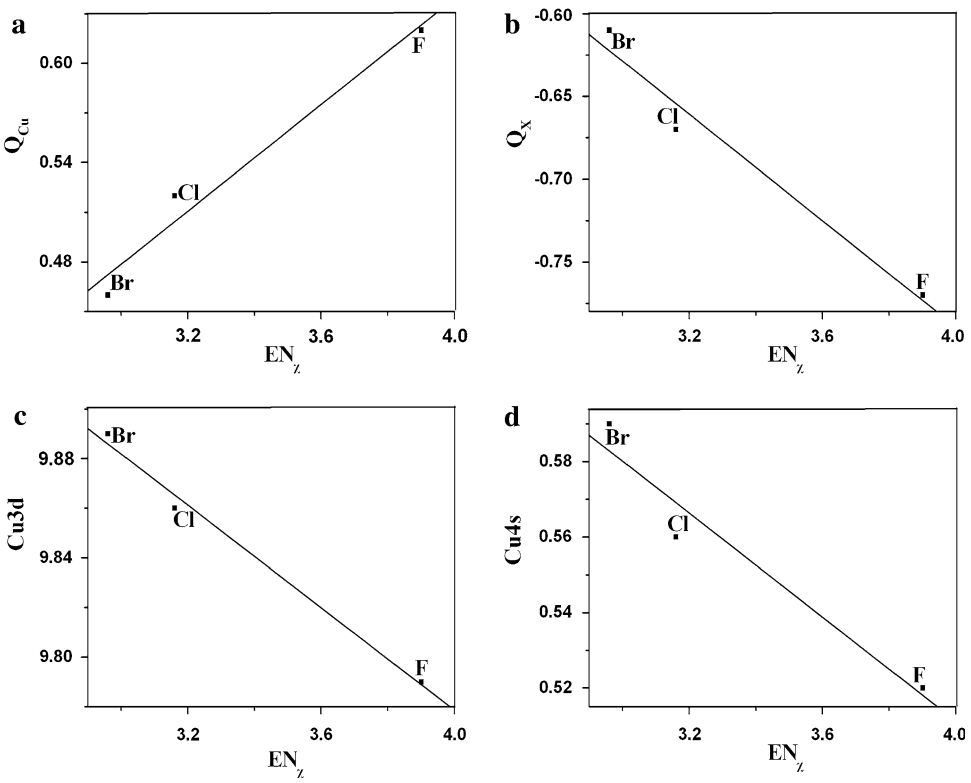

Fig. 6 Correlation of electronegativity EN_χ of atom and, **a** effective charge of Cu, Q_{Cu}; **b** effective charge of X, Q_X; **c** population of Cu3d; **d** population of Cu4s in XeCuX

3.4 Variation of the halogen atom

3.4.1 The M–X bond length

For XeMX (M = Au, Ag, Cu; X = F, Cl, Br) system, if R_X is the effective radius of the halogen atom, the M–X bond length varies with the transformation from F to Br. The electronegativity EN_χ is strongly coupled to the valence radii of X. The results are listed in Table 5. The correlation between R_{M-X} and EN_χ is shown in Fig. 2. The correlation between electronegativity (EN_χ) of X and R_{M-X} is linear. The line in Fig. 2 is probably due to the different overall charges Q.

3.4.2 HOMO-LUMO gap

The HOMO-LUMO gaps are displayed in Table 5, too. As to be expected, they correlate with the EN_χ of the halogen atom X (Fig. 3), of course along the line depending on the overall charge Q. The frontier orbital HOMO-LUMO energy gaps may correlate with the stability of the systems. From our calculations, we find that with X = F, the XeAuF become the most stable molecule (Table 5).

3.4.3 The M-charge Q_M, X-charge Q_X, Mns and M(n−1)d population

The correlations between Q_M, Q_X, the Mns, M(n−1)d population and the electronegativity EN_χ of atom X is shown in Figs. 4, 5, 6. The bigger the electronegativity (EN_χ) of X, the larger the effective charge Q_M and Q_X, the larger the hole in the M(n−1)d shell, and the fewer electron in the Mns shell, the stronger Xe–M interaction.

3.5 Chemical deformation densities

The charge density distribution provides valuable information about the nature of bonding or nonbonding interactions in various molecular systems. Belpassi et al. [54] have carried out the topological analysis of the electronic density upon formation of the Ng–Au bond and the corresponding charge-transfer curves. The electronic density mainly developed in the framework of the theory of atoms in molecules (AIM) of Bader et al. [62]. They found: "the Ng–M bond is a pronounced charge accumulation in the middle region between the Ng and Au nuclei, delimited on both sides by a zone of charge depletion particularly

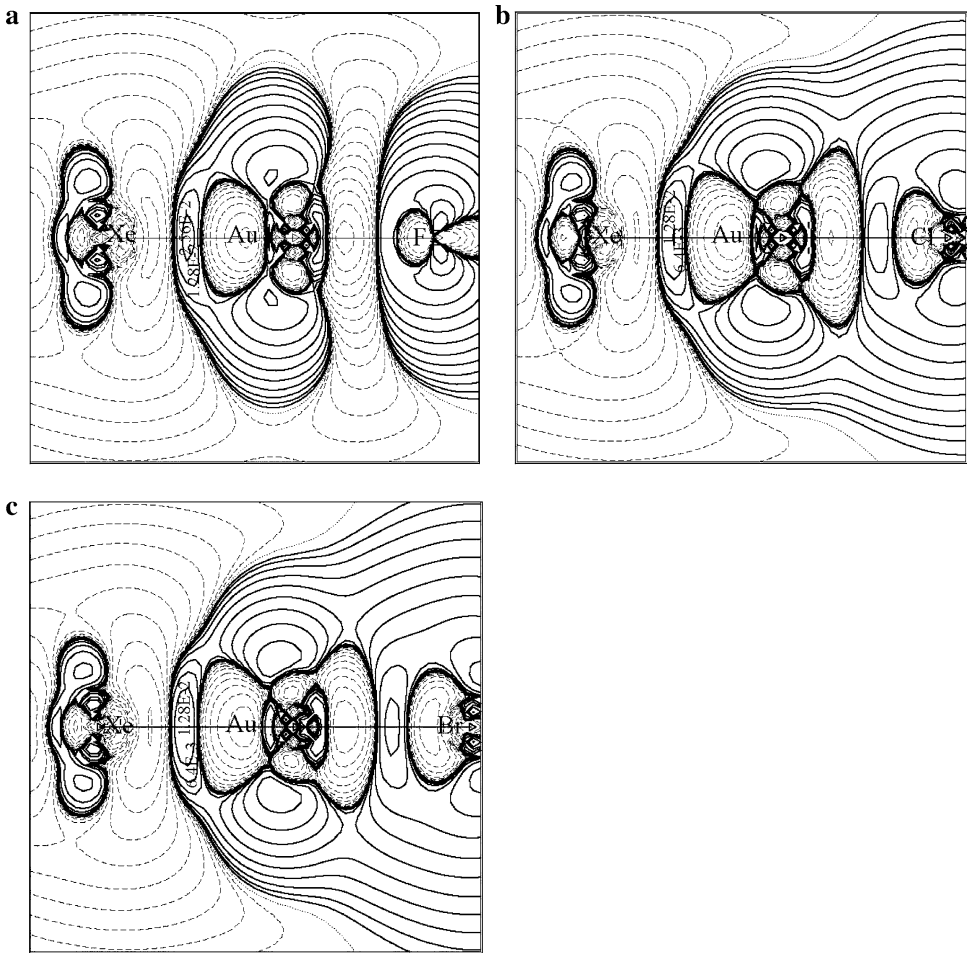

Fig. 7 Electron density difference $\Delta\rho$ (e/Å^3) plots at Xα level, **a** XeAuF; **b** XeAuCl; **c** XeAuBr; along the plane of three atoms. Contour line values are $\pm 0.01 \times 2^n$ eÅ^{-3} (n = 0, 1, 2, …); negative contour lines are *dashed*

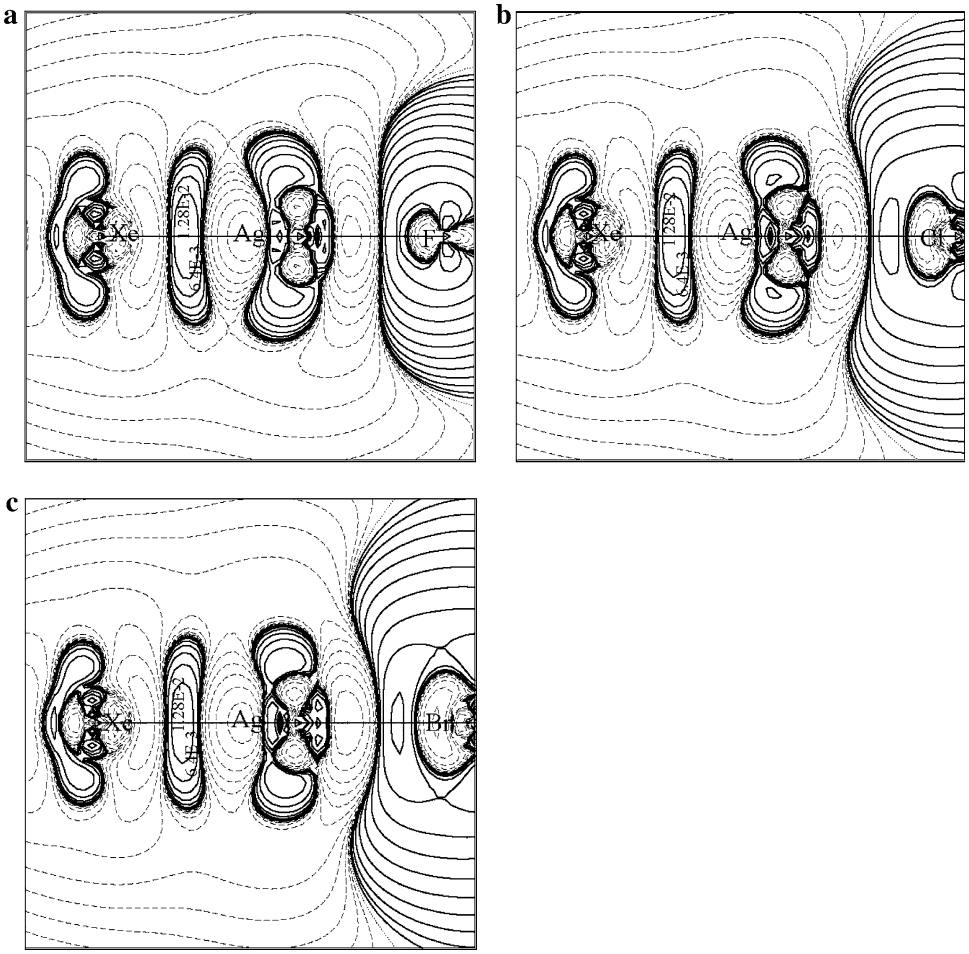

Fig. 8 Electron density difference $\Delta\rho$ (e/Å^3) plots at Xα/TZ2P level, **a** XeAgF; **b** XeAgCl; **c** XeAgBr; along the plane of three atoms. Contour line values are $\pm 0.01 \times 2^n$ eÅ^{-3} ($n = 0, 1, 2, \ldots$); negative contour lines are *dashed*

marked at the noble gas". They concluded that the Ng–Au interaction is a polar covalent bond.

For the title compounds, we want to calculate the chemical deformation density which in the XeMX system to study the Xe–M bond. Dalton [63] introduced the concept of atoms in chemistry as building blocks of matter, which retain their individuality and spherical shape to a large extent when they form compounds. It is often implicitly assumed or explicitly stated that independent atoms can only possess spherically symmetric charge distributions. A common practice is to compare the electron density distribution in molecules and crystals with a reference density, which is the superposition of densities of the independent atoms in their spherically symmetric ground states. The above mentioned density pattern is usually called the "deformation density". It is believed that any deviation from sphericity of the charge distribution of AIM or crystals is an indication of the chemical forces between them.

Figures 7, 8, 9 give the deformation density maps for XeMX (M = Au, Ag, Cu; X = F, Cl, Br). Solid contours mean electronic density increase, dashed contours mean electronic density decrease. Figures 7, 8, 9 display about +0.01–0.02 e/Å^3 maximum density increase between the Xe and M atoms in XeMX system. However, the values of all the maximum density are very small and change little from molecule to molecule, making any sharp distinction in the nature of the bond for the three metal atoms. The deformation density can not associate with the Xe–M interactions directly. The regions of density increased are, therefore, the regions to which charge is transferred relative to the separated atoms to obtain a state of electrostatic equilibrium and hence a chemical bond. From this point of view, a density difference map provides us with a picture of the "bond density".

4 Conclusion

In this work, ab initio CCSD(T) and DFT methods have been performed to explore the geometric structure, electronic structure, HOMO-LUMO gap and weak noble

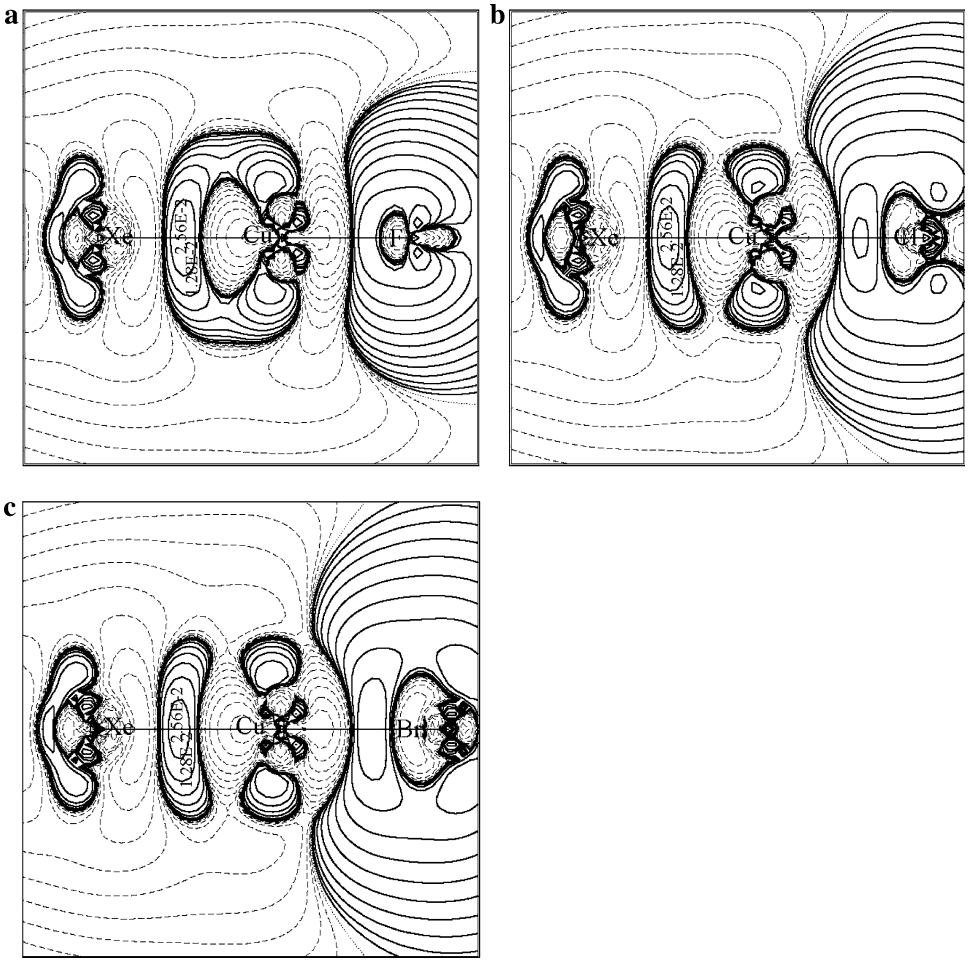

Fig. 9 Electron density difference $\Delta\rho$ (e/Å^3) plots at Xα/TZ2P level, **a** XeCuF; **b** XeCuCl; **c** XeCuBr; along the plane of three atoms. Contour line values are $\pm 0.01 \times 2^n$ eÅ^{-3} ($n = 0, 1, 2, \ldots$); negative contour lines are *dashed*

gas-noble metal interaction. The key conclusions are as follows:

1. For XeMX (M = Au, Ag, Cu; X = F, Cl, Br) system, the simplest local Xα functional and ab initio CCSD(T) methods can reproduce the geometric structures fairly well as compared to experimental results, within 2 pm. With nonlocal gradient correlations, DFT overestimated them. In all the species except for XeAuF, the Xe–M distances are between the covalent limit and van der Waals limit. For XeAuF, the Xe–Au distance is less than the covalent limit for about 3 pm.
2. The NBO charges and populations are investigated. Since Xe5p and M($n-1$)d shell is not completely closed shell, the weak rare gas-noble metal interaction occurs. At the same time, a net charge transfer of $\sim$0.15 electron from Xe to MX, as well as valence molecular orbital with fully shared electron density between Xe and M. There is thus strong evidence of rare gas-noble metal chemical bonding in these complexes that is also indicated by interference densities of up to +0.01–0.02 e/Å^3 between the interacting Xe–M atoms.
3. The weak rare gas-noble metal interaction is decomposed and analyzed. The Xe–M interaction in XeMX as X is altered from Br to F. And for the same X atom, we observed the increasing strength of the Xe–M interaction in XeMX is along with the order: $E_{\text{Xe–Au}} > E_{\text{Xe–Cu}} > E_{\text{Xe–Ag}}$. The electronegativity of halogen atom X correlate well with the Xe–M distances, the HOMO-LUMO gap, the charge on the M, X atoms and the population of Mns, M($n-1$)d shells.

Acknowledgments We acknowledge the financial supports by China Postdoctoral Foundation and Postdoctoral Foundation of Jiangsu Province. We would like to thank Prof. Dr. Shu-Guang Wang for providing us with the ADF2008 software, and Shanghai Jiao Tong University Computing and Network Services for computer time.

References

1. Pauling L (1933) J Am Chem Soc 55:1895. doi:10.1021/ja01332a016
2. Bartlett N (1962) Proc Chem Soc 112:218

3. Gerber RB (2004) Annu Rev Phys Chem 55:55. doi:10.1146/annurev.physchem.55.091602.094420
4. Pettersson M, Khriachtchev L, Lundell J, Räsänen M (2005) In: Meyer G, Naumann D, Wesemann L (eds) Inorganic chemistry in focus II. Wiley, Weinheim, pp 15–34
5. Christe KO (2001) Angew Chem Int Ed Engl 40:1419. doi:10.1002/1521-3773(20010417)40:8<;1419::AID-ANIE1419>;3.0.CO;2-J
6. Evans CJ, Gerry MCL (2000) J Chem Phys 112:1321. doi:10.1063/1.480684
7. Evans CJ, Gerry MCL (2000) J Chem Phys 112:9363. doi:10.1063/1.481557
8. Evans CJ, Lesarri A, Gerry MCL (2000) J Am Chem Soc 122:6100. doi:10.1021/ja000874l
9. Evans CJ, Rubino DS, Gerry MCL (2000) Phys Chem Chem Phys 2:3943. doi:10.1039/b004352o
10. Reynard LM, Evans CJ, Gerry MCL (2001) J Mol Spectrosc 206:33. doi:10.1006/jmsp.2000.8286
11. Walker NR, Reynard LM, Gerry MCL (2002) J Mol Struct 612:109. doi:10.1016/S0022-2860(02)00081-9
12. Cooke SA, Gerry MCL (2004) J Am Chem Soc 126:17000. doi:10.1021/ja044955j
13. Cooke SA, Gerry MCL (2004) Phys Chem Chem Phys 6:3248. doi:10.1039/b404953p
14. Thomas JM, Walker NR, Cooke SA, Gerry MCL (2004) J Am Chem Soc 126:1235. doi:10.1021/ja0304300
15. Michaud JM, Cooke SA, Gerry MCL (2004) Inorg Chem 43:3871. doi:10.1021/ic040009s
16. Michaud JM, Gerry MCL (2006) J Am Chem Soc 128:7613. doi:10.1021/ja060745q
17. Ghanty TK (2005) J Chem Phys 123:074323. doi:10.1063/1.2000254
18. Ghanty TK (2006) J Chem Phys 124:124304. doi:10.1063/1.2173991
19. Seidel S, Seppelt K (2000) Science 290:117. doi:10.1126/science.290.5489.117
20. Wang SG, Schwarz WHE (2004) J Am Chem Soc 126:1266. doi:10.1021/ja035097e
21. Fang H, Wang SG (2006) J Mol Struct 773:15. doi:10.1016/j.theochem.2006.06.034
22. Fang H, Wang SG (2007) J Phys Chem A 111:1562. doi:10.1021/jp064656b
23. Fang H, Wang SG (2007) J Mol Model 13:255. doi:10.1007/s00894-006-0156-5
24. Fang H, Wang SG, Zhang XG (2009) Int J Quantum Chem 109:526
25. Pyykkö P (1995) J Am Chem Soc 117:2067. doi:10.1021/ja00112a021
26. Schröder D, Schwarz H, Hrusak J, Pyykkö P (1998) Inorg Chem 37:624. doi:10.1021/ic970986m
27. Yousef A, Shretha S, Breckenridge WH (2007) J Chem Phys 127:154309. doi:10.1063/1.2774977
28. Frisch MJ, Trucks GW, Schlegel HB, Scuseria GE, Robb MA, Cheeseman JR, Zakrzewski VG, Montgomery JA Jr, Stratmann RE, Burant JC, Dapprich S, Millam JM, Daniels AD, Kudin KN, Strain MC, Farkas O, Tomasi J, Barone V, Cossi M, Cammi R, Mennucci B, Pomelli C, Adamo C, Clifford S, Ochterski J, Petersson GA, Ayala PY, Cui Q, Morokuma K, Malick DK, Rabuck AD, Raghavachari K, Foresman JB, Cioslowski J, Ortiz JV, Stefanov BB, Liu G, Liashenko A, Piskorz P, Komaromi I, Gomperts R, Martin RL, Fox DJ, Keith T, Al-Laham MA, Peng CY, Nanayakkara A, Gonzalez C, Challacombe M, Gill PMW, Johnson B, Chen W, Wong MW, Andres JL, Gonzalez C, Head-Gordon M, Replogle ES, Pople JA (2004) Gaussian 03, Rev. E. 01. Gaussian, Inc, Wallingford
29. Te Velde G, Bichelhaupt FM, Baerends EJ, Fonseca Guerra C, Van Gisbergen SJA, Snijders JG, Ziegler T (2001) J Comput Chem 22:931. doi:10.1002/jcc.1056
30. Slater JC (1951) Phys Rev 81:385. doi:10.1103/PhysRev.81.385
31. Slater JC (1974) Quantum theory of molecules and sloids, vol 4. McGraw-Hill, New York
32. Gaspar R (1954) Acta Phys 3:263
33. Schwarz K (1972) Phys Rev B 5:2466. doi:10.1103/PhysRevB.5.2466
34. Vosko SH, Wilk L, Nusair M (1980) Can J Phys 58:1200
35. Becke AD (1988) J Chem Phys 88:2547. doi:10.1063/1.454033
36. Perdew JP (1986) Phys Rev B 34:7406. doi:10.1103/PhysRevB.34.7406
37. Perdew JP (1992) Phys Rev B 46:6671. doi:10.1103/PhysRevB.46.6671
38. Te Velde G, Baerends EJ (1992) J Comput Phys 99:84. doi:10.1016/0021-9991(92)90277-6
39. Rosen A, Lindgren I (1968) Phys Rev 176:114. doi:10.1103/PhysRev.176.114
40. Van Lenthe E, Ehlers AE, Baerends EJ (1999) J Chem Phys 110:8943. doi:10.1063/1.478813
41. Van Lenthe E, Baerends EJ, Snijders JG (1994) J Chem Phys 101:9783. doi:10.1063/1.467943
42. Van Lenthe E, Snijders JG, Baerends EJ (1996) J Chem Phys 105:6505. doi:10.1063/1.472460
43. Van Lenthe E (1996) Int J Quantum Chem 57:281. doi:10.1002/(SICI)1097-461X(1996)57:3<;281::AID-QUA2>;3.0.CO;2-U
44. Lensch C, Jones PG, Sheldrick GM (1982) Z Naturforsch [C] 37b:944
45. Kendall RA, Dunning TH, Harrison RJ et al (1992) J Chem Phys 96:6796. doi:10.1063/1.462569
46. Woon DE, Dunning TH Jr (1993) J Chem Phys 98:1358. doi:10.1063/1.464303
47. Wilson AK, Woon DE, Peterson KA, Dunning TH Jr (1999) J Chem Phys 110:7667. doi:10.1063/1.478678
48. Peterson KA, Figgen D, Goll E, Stoll H, Dolg M (2003) J Chem Phys 119:11113. doi:10.1063/1.1622924
49. Peterson KA, Puzzarini C (2005) Theor Chem Acc 114:283. doi:10.1007/s00214-005-0681-9
50. Feller D (1996) J Comput Chem 17(13):1571
51. Schuchardt KL, Didier BT, Elsethagen T, Sun L, Gurumoorthi V, Chase J, Li J, Windus TL (2007) J Chem Inf Model 47(3):1045. doi:10.1021/ci600510j
52. Lovallo CC, Klobukowski M (2003) Chem Phys Lett 368:589. doi:10.1016/S0009-2614(02)01913-9
53. Lantto P, Vaara J (2006) J Chem Phys 125:174315. doi:10.1063/1.2363371
54. Belpassi L, Infante I, Tarantelli F, Visscher L (2008) J Am Chem Soc 130:1048. doi:10.1021/ja0772647
55. Mizoguchi A, Endo Y, Ohshima Y (1998) J Chem Phys 109:10539. doi:10.1063/1.477754
56. Ohshima Y, Iida M, Endo Y (1990) J Chem Phys 92:3990. doi:10.1063/1.457810
57. Buxton LW, Campbell EJ, Keenan MR, Balle TJ, Flygare WH (1981) Chem Phys 54:173. doi:10.1016/0301-0104(81)80232-7
58. Baiocchi FA, Dixon TA, Joyner CH, Klemperer W (1981) J Chem Phys 75:2041. doi:10.1063/1.442322
59. Ziegler T (1984) J Am Chem Soc 106:5901. doi:10.1021/ja00332a025
60. Ziegler T, Rauk A (1977) Theor Chim Acta 46:1
61. Famiglietti C, Baerends EJ (1981) J Chem Phys 62:407. doi:10.1016/0301-0104(81)85135-X
62. Bader RFW (1991) Atoms in molecules. A quantum theory. Cambridge University Press, Oxford
63. Dalton J (1803) Mem Lit Philos Manchester II 1:271